arXiv:astro-ph/0306153v2 20 Jun 2003

HII regions in the spiral galaxy NGC 3389

Hamed Abdel-Hamid[1,2] and Sang-Gak Lee[1]

1- Astronomy Program, SEES, Seoul National University, Seoul 151-742, Korea

2- National Research Institute of Astronomy and Geophysics, Cairo, Egypt

hamed@astro.snu.ac.kr, sanggak@astrosp.snu.ac.kr

and

Peter Notni

Astrophysikalisches Institut Potsdam, D-14482 Potsdam, Germany

pnotni@aip.de

ABSTRACT

CCD observations in V, I and H_α for NGC 3389 are used to present photometry of 61 HII regions. Their α and δ positions, diameters and their absolute luminosities have been determined. The luminosity and size distribution functions of the HII regions in NGC 3389 are discussed.

Subject headings: galaxies:spiral-HII regions—galaxies:individual (NGC 3389)

1. Introduction

NGC 3389 is a spiral galaxy, classified by de Vaucouleurs et al. (1991) as SA galaxy and by Sandage and Tammann (1981) as Sc galaxy. NGC 3389 is one of the Leo triplet with the galaxies NGC 3384 and NGC 3379. The lack of detailed photometric studies for NGC 3389 and its normal undistorted morphology, although it lies in a group of galaxies, motivate us to do the photometry of NGC 3389 and study its stellar population properties. The basic parameters of NGC 3389 are given in the Table 1.

HII regions in galaxies are powered by the newly formed stars, therefore they give the clues for the recent star formation in galaxies. The total H_α luminosity can be used to quantify their current star formation rate. Therefore we concern firstly with the investigation of the HII region properties of NGC 3389; their luminosity and size distributions.

This is the first CCD work on the HII regions of NGC 3389. Hodge and Kennicutt (1983) presented the off-set positions for 50 identified HII regions in NGC 3389 in their photographic surveys of the HII regions in galaxies, while Kennicutt and Kent (1983) gave the total integrated H_α flux and luminosity for the galaxy.

2. Observations and data reduction

The V, I and H_α CCD observations of NGC 3389 were obtained using 1.23 m telescope of Calar Alto observatory on 5-6 February 1995 with a Tek CCD with 1024 × 1024 pixels with a pixel scale of $0.502''$ pixel^{-1}. The sky was photometric with seeing varying from $0.7''$ to $1.2''$ during the night. Four H_α frames were taken with H_α interference filter of central bandpass at 6580 $\mathring{A}$ and a FWHM of 100 $\mathring{A}$. Four frames in V filter and three frames in I filter were observed. Table 2 gives the log of the observations. All data reduction were done using the image processing program MIDAS. The standard image processing routine has been done, then all frames were carefully aligned using the position of the common foreground stars in the frames. The sky background was measured using MIDAS task FIT/FLATSKY with cursor area offset from the galaxy in the frame margin. After sky subtraction, the cosmic ray effects are removed by median filter. A weighted mean image for each filter was computed. In order to get an accurate continuum level we have choosen two continuum bands on either side of H_α; V and I are used. The fluxes of the selected stars in the three bands (I, V and H_α) were measured, then correlations among them get the H_α continuum level. Then the H_α image was corrected for the continuum contribution. For flux calibration, we compare the integrated measurements within an aperture whose diameter equal to three arcminutes, which contains the entire visible disk of NGC 3389 to a limiting surface brightness of 25 mag/arcsec^2 with the total absolute luminosity given by Bell and Kennicutt (2001). This total integration normalized by the total absolute luminosity quoted by Bell and Kennicutt (2001), for the same diameter size ($3'$), to get the observed measurements in units of erg s^{-1}. The absolute flux has been measured with the same H_α filter specification (λ 6580/100 $\mathring{A}$) like that of ours. Bell and Kennicutt (2001) used to convert the fluxes to luminosity the adopted distance of 24 Mpc refering to Shanks (1997).

3. HII regions identification

The Figure 1 shows the continuum-subtarcted Hα image of NGC 3389. A visiual identification of the HII regions was firstly done, by displaying the continuum-subtarcted Hα image with different scaling factors and measure the boundaries at the discernable level. To

measure the contour dimensions of each HII region (dx and dy) using a graphically interface precedure within MIDAS was used. However if the HII regions are crowded or lie in a diffuse bright background the largest closed contour is used to measure the HII region boundary. From both methods we fixed dimensions of the HII regions. In some cases it was needed to justifity the aperture radius by hand. The aperture radius used for the flux integration was calculated as follows:

$$r = (\sqrt{dx^2 + dy^2})/2 \tag{1}$$

The aperture radius used to estimate the backgroud flux in the proximity of each HII region is varied according to how much HII regions are crowded.

Figures 1 and 2 illustrate the positions of 61 HII regions in NGC 3389 in comparison with those of Hodge and Kennicutt (1983); Hodge provided the off-set positions of HII regions from the center of NGC 3389 and a map of NGC 3389 by private communication. We find a good agreement between our position measurments and their position data for 40 objects. The rest ten HII regions of Hodge and Kennicutt (1983) have no counterparts in our data. These ten HII regions may lie below our identification criterion, their off-set positions and identification names are given in Table 3. Twenty one HII regions are newly identified.

The integrated flux and the background flux for each HII region are measured, then the flux corrected for the background to give the net flux. The main source of error in the net fluxes are due to either the estimation of the background or the inaccurate estimate of the boundaries, or both. To estimate the uncertainties in the flux measurements multiple trials have been done to measure the flux of some individuals HII regions. We found statistically that the uncertainities in the measured fluxes vary from less than 10% for the isolated regions to 20% for the crowded regions.

The measured H_α fluxes are corrected for Galactic extinction, $A(0.65\mu m) = 0.073$ mag (Schlegel et al. 1998). To remove the contamination by the [NII] emission lines in the measured H_α fluxes, the total fluxes were multiplied by a factor of 0.75 according to Kennicutt (1983); the factor gave the average ratio of $H_\alpha/(H_\alpha+[NII])$ in the spirals. They have used the same filter bandpass at 6580 $\mathring{A}$ and FWHM of 100 $\mathring{A}$ in their measurments for galaxies with radial velocities under 3000 $\mathrm{km\,s^{-1}}$as NGC 3389. Sixty one HII regions were identified, and the equatorial coordinates of their positions, the diameters in parsec, the logarithmical lumnosities and the corresponding Hodge & Kennicutt (1983) identifications (HK-ID) are listed in Table 4.

4. The Luminosity Function

The H_α luminosity of the HII regions in NGC 3389 spans a range $L(H_\alpha) \approx 3\times10^{37}$-$6\times10^{39}$ erg s^{-1}. This $L(H_\alpha)$ luminosity range is more frequent in Sa-Sb galaxies (see for example in Thilker et al. 2002). The HII regions with $L(H_\alpha)$ luminosity higher than 10^{39} erg s^{-1} are found in late-type (Sc-Irr) normal galaxies or in interacting galaxies (Kennicutt et al. 1989). The luminosites of the 61 HII regions are binned in logarithmic interval of 0.2 dex and ploted in Figure 3.

In the Figure 3, our LF data is compared with that of Feinstein (1997) on the Sb spiral galaxy NGC 6384. The HII regions in both galaxies exhibit nearly the same $L(H_\alpha)$ range, but the number of the HII regions of NGC 6384 is about four times larger than that of NGC 3389. The reason for that is the absolute blue luminosity of NGC 6384 (M_B=-21.31) is approximately four times that of NGC 3389. A mimic relation is founded on NGC 6822 by Hodge et al. (1989).

In order to fit the luminosity distribution of the HII regions independantly of the choosing the LF bin size, the cumulative luminosity distribution have been done following Feinstein (1997). The cumulative LF is presented in Figure 4 in comparison with that of NGC 6384 (Feinstein 1997), both LFs for the two galaxies normalized by their number of the HII regions at log(L) of 38.6. The LFs are in agreement at the luminosities $\log(L) \leq 39.0$, while they are incongruent at higher luminosities $\log(L) > 39.0$. This is due to NGC 6384 has 49 HII regions with luminosities higher than 39.0 (log) while NGC 3389 contains only 4 HII regions. The two galaxies have different absolute blue luminosities as well as different spiral types. This result may confirm that NGC 3389 is neither Sc spiral nor an interacting galaxy.

The straight line in the Figure 4 gives the best fit for all data points of NGC 3389 LF, which correspondes to a power law in the form:

$$dN = AL^{\alpha}dL \tag{2}$$

With a power index α=-1.95±0.24, which is in agreement with α = -2.0±0.2 for Sa-Sb galaxies quoted by Banfi et al. (1993) for a sample of 22 spirals and with α = -2.0±0.5 for a sample of 30 spirals (Kennicutt et al. 1989).

5. Diameter distribution

Figure 5 shows the diameter distribution for the HII regions of NGC 3389. The number of HII regions with diameter greater than a given diameter value plotted as a function of diameter. The data fit an exponential law, as proposed by the previous works from Van

den Berg (1981), Hodge (1983), Hodge (1987) and many others. The exponential law in the form $N = N_\circ e^{-D/D_\circ}$. We obtain $D_\circ = 200 \pm 7$ pc, which is in agreement with that given by Hodge (1987); 180 pc for NGC 3389, if the smallest diameters were ignored in fitting.

6. Summary

We have identified 61 HII regions in the spiral galaxy NGC 3389. The positions of fourty of them are identical with those in Hodge & Kennicutt (1983) and 21 are newly identified. The diameters and the fluxes of 61 HII regions are measured for NGC 3389 for the first time. The H_α luminosities of HII regions span a range from 3×10^{37} to 6×10^{39} erg s^{-1} as those in most Sa-Sb galaxies. The luminosity function fits well a power law with a power index is in agreement with that for early spiral galaxies. In a forthcoming paper, we will discuss the ionization sources of the HII regions and star formation activity in NGC 3389.

This work is financially supported by SEES-BK21 grant, Korean Government. Abdel-Hamid is very grateful to BK21 and School of Earth and Environmental Science (Astronomy Program) at Seoul National University for their support and good hospitality. We are grateful to P. Hodge for providing us his HII regions data for NGC 3389.

REFERENCES

Banfi, R., Chincarini, G., & Henry, R. B. C. 1993, A&A, 280, 373

Bell, E., & Kennicutt, R. C., Jr. 2001, ApJ, 548, 693

de Vaucouleurs, G., de Vaucouleurs, A., Corwin, H. G.Jr., Buta, R. J., Paturel, G., & Fouque, P. 1991, The 3rd Reference Catalog of Bright Galaxies, Spring-Verlag, New York.

Feinstein, C. 1997, ApJS, 112, 29

Hodge, P. W. 1983, AJ, 88, 1323

Hodge, P. W. 1987, PASP, 99, 915

Hodge, P.W., & Kennicutt, R. C., Jr. 1983, AJ, 88, 296

Hodge, P.W., Lee, M. G., & Kennicutt, R. C., Jr. 1989, PASP, 101, 32

Kennicutt, R. C., Jr., Edgar, B. K., & Hodge, P. W. 1989, ApJ, 337, 761

Kennicutt, R. C., Jr., & Kent, S. M. 1983, AJ, 88, 109

Kennicutt, R. C., Jr. 1983, ApJ, 272, 54

Sandage, A., & Tamman, G. 1981, A revised Shapley-Ames Catalog of Bright Galaxies (Washington:Carneige Institution of Washington).

Schlegel, D. J., Finkbeiner, D. P. & Davis M. 1998, ApJ, 500, 525.

Shanks, T. 1997, MNRAS, 290, L77.

Thilker, D. A., Walterbos R. A. M., Braun R., & Hoopes C. G. 2002, ApJ, 124, 3134.

Tully, R.B. 1988, Nearby Galaxies Catalog (Cambridge University Press).

van den Berg, S. 1981, AJ, 86, 1464.

This preprint was prepared with the AAS LaTeX macros v5.0.

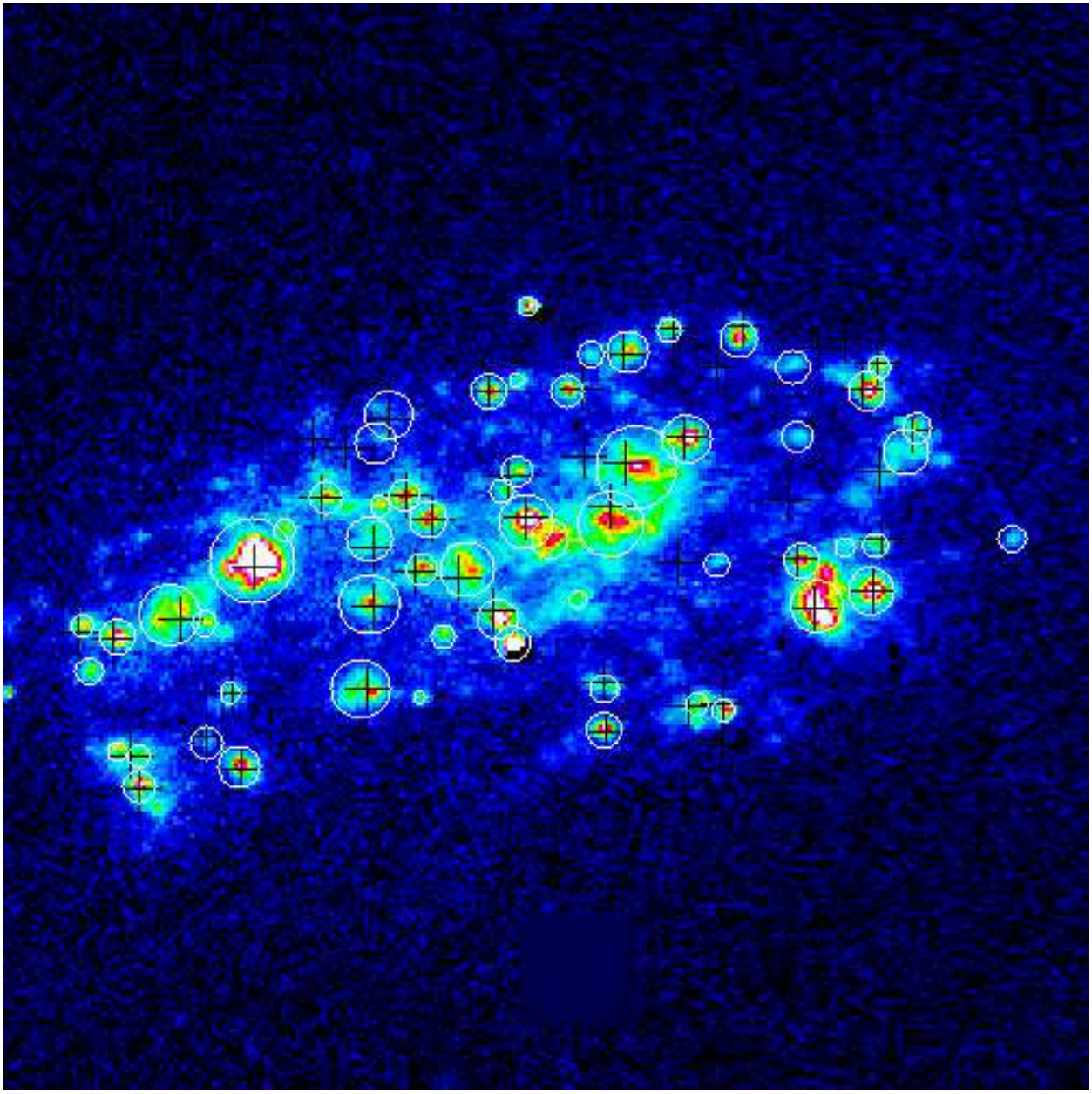

Fig. 1.— Continuum subtracted H_α image for NGC 3389 with HII regions of this study (ellipses) and those of Hodge& Kennicutt (1983) (crosses).

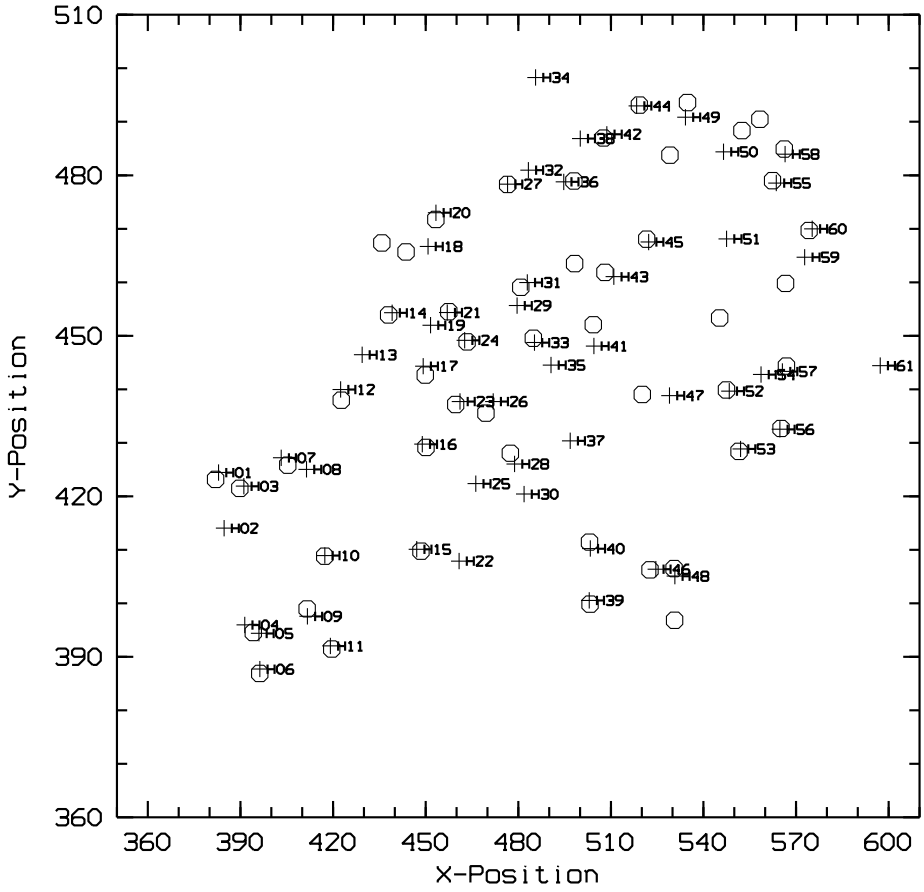
510
480
450
420
390
360
Y-Position
360
390
420
450
480
510
540
570
600
X-Position
H34
H44
H49
H42
H50
H58
H32
H27
H36
H55
H20
H60
H45
H51
H18
H59
H31
H43
H29
H14
H21
H19
H24
H33
H41
H13
H17
H35
H61
H12
H23
H26
H47
H52
H56
H16
H37
H53
H07
H28
H01
H08
H03
H25
H30
H02
H10
H15
H22
H40
H46
H48
H39
H09
H04
H05
H11
H06

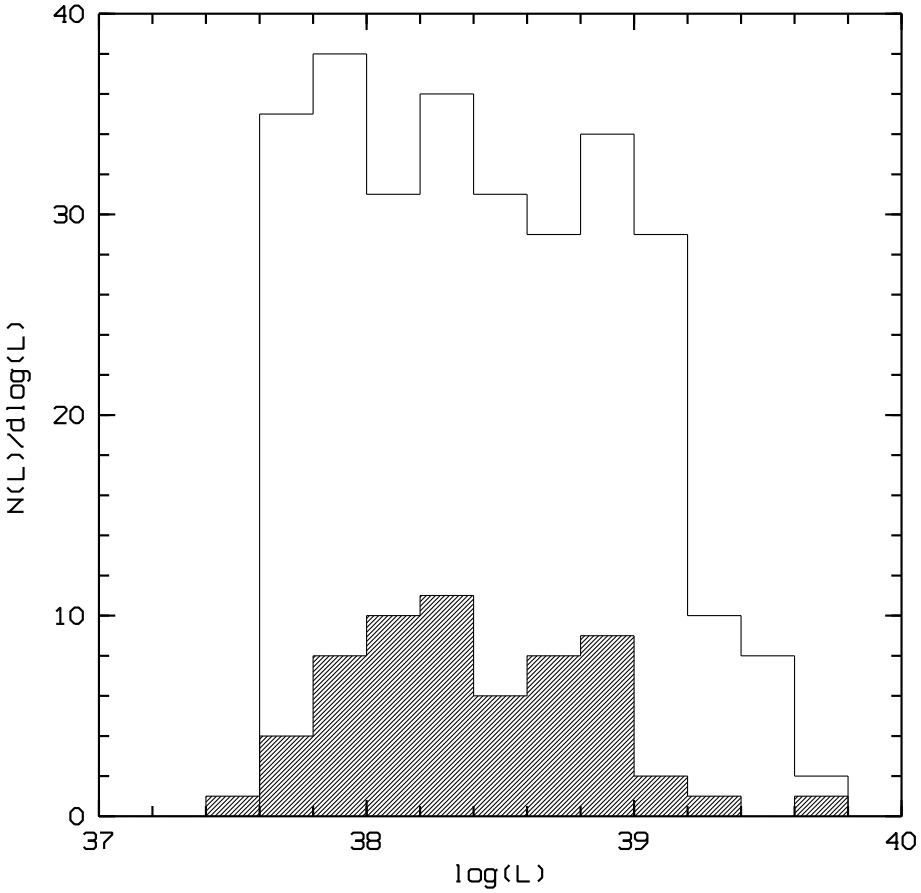
40
30
20
10
0
N(L)/dlog(L)
37
38
39
40
log(L)

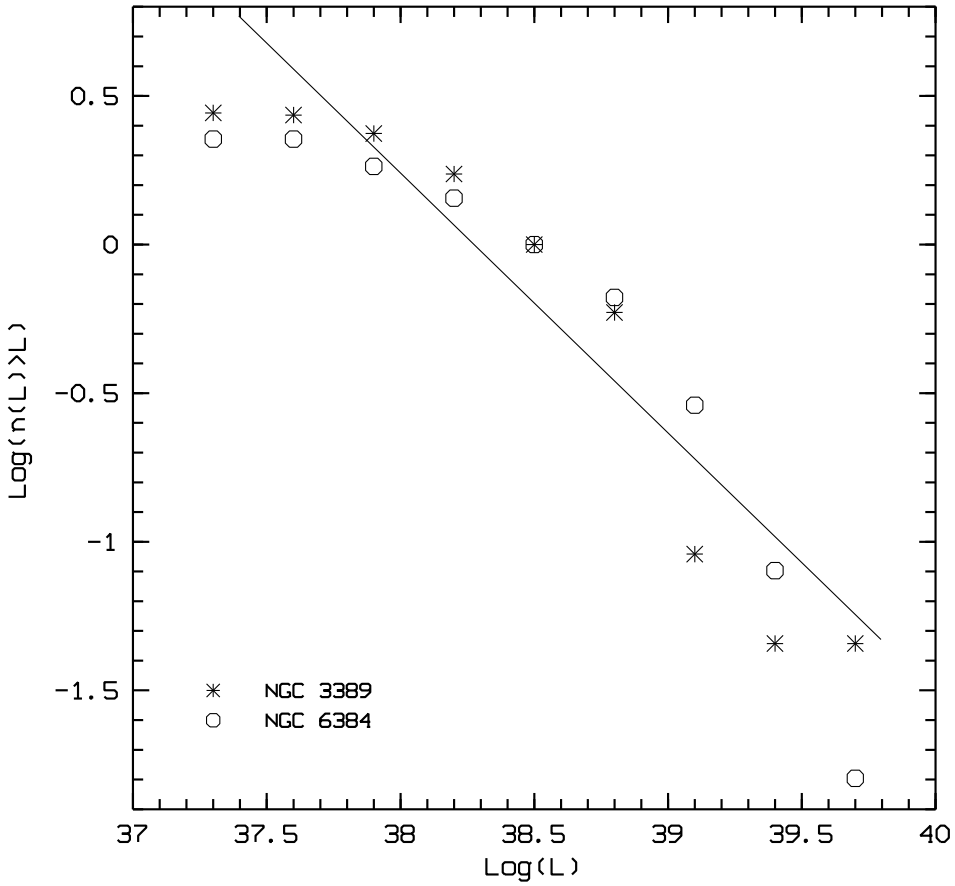
0.5
0
-0.5
-1
-1.5
Log(n(L)>L)
37
37.5
38
38.5
39
39.5
40
Log(L)
NGC 3389
NGC 6384

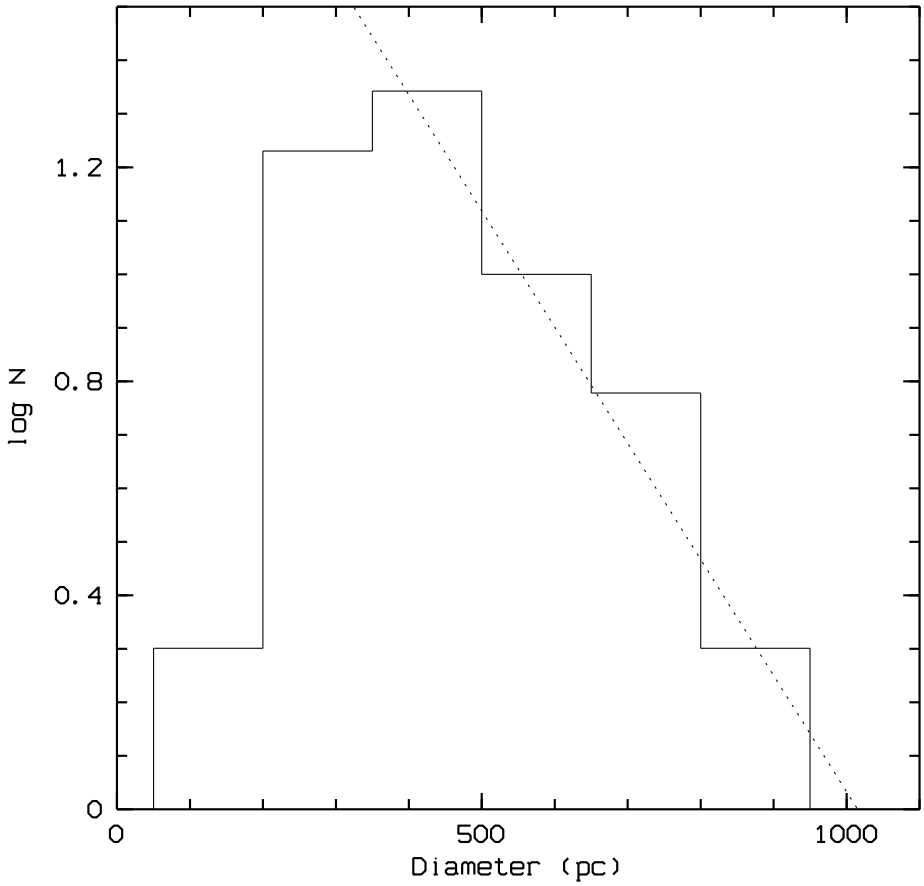
1.2
0.8
0.4
0
log N
0
500
1000
Diameter (pc)

Table 1: Basic Parameters for NGC 3389

R.A. (2000.0)	$10\ ^{h}\ 48\ ^{m}\ 28\ ^{s}$	
Dec (2000.0)	$12\ ^{d}\ 31\ ^{\prime}\ 59\ ^{\prime\prime}$	
Type	SA(s)	de Vaucouleurs et al. 1991
Diameters	2.8×1.3 arcminutes	
radial Velocity	1306±6 km/sec	de Vaucouleurs et al. 1991
M_B	-19.82	Tully 1988
Lα	1.08×10^{41}erg/sec	D=24 Mpc, Bell & Kennicutt 2001
Lα aperture size	3 arc minutes	

Table 2: Log of the Observations

Filter	V	I	H_α
Exposure Time in second	100, 500, 500, 600	500, 500, 500	1000, 1000, 1000, 1500
Date	February 5-6, 1995		
Observer	P. Notni		

Table 3. Un-identified Hodge and Kennicutt (1983) HII regions

KH-ID	X-off	Y-off
10	031	010
12	027	009
25	-001	007
32	-012	-006
36	-017	017
37	-017	-028
40	-025	001
43	-029	019
44	-032	020
47	-036	004

Table 4. HII region in NGC 3389

Name	R.A.(2000.0)	Dec. (2000.0)	Diameter (pc)	log L (erg/sec)	HK-ID
H01	$10^h48^m28.80^s$	$12^d31'49.67''$	277	38.24	1
H02	10 48 28.96	12 31 44.43	370	38.29	-
H03	10 48 28.58	12 31 48.38	472	38.74	2
H04	10 48 29.11	12 31 35.33	264	38.11	-
H05	10 48 28.99	12 31 34.54	293	37.90	3
H06	10 48 29.12	12 31 31.18	442	38.61	4
H07	10 48 28.08	12 31 51.04	815	38.97	5
H08	10 48 27.85	12 31 49.95	328	37.98	-
H09	10 48 28.41	12 31 36.13	440	37.69	6
H10	10 48 27.98	12 31 41.84	279	38.03	7
H11	10 48 28.27	12 31 33.34	555	38.78	8
H12	10 48 27.18	12 31 57.46	1138	39.80	9
H13	10 48 26.82	12 32 00.72	302	37.88	-
H14	10 48 26.33	12 32 04.66	421	38.38	11
H15	10 48 26.98	12 31 42.42	798	38.96	13
H16	10 48 26.52	12 31 52.30	799	38.82	14
H17	10 48 26.20	12 31 59.63	591	38.41	15
H18	10 48 25.70	12 32 10.90	567	37.54	-
H19	10 48 25.97	12 32 03.48	267	37.96	-
H20	0 48 25.48	12 32 14.06	642	38.17	16
H21	10 48 25.74	12 32 04.67	404	38.46	17
H22	10 48 26.57	12 31 41.29	165	37.70	-
H23	10 48 25.95	12 31 56.30	416	38.46	18
H24	10 48 25.66	12 32 02.06	490	38.63	19
H25	10 48 26.09	12 31 48.58	331	38.18	-
H26	10 48 25.59	12 31 56.29	724	38.82	20
H27	10 48 24.61	12 32 16.74	468	38.61	22
H28	10 48 25.60	12 31 50.42	549	38.33	21
H29	10 48 24.97	12 32 05.32	331	37.70	-
H30	10 48 25.61	12 31 47.59	452	38.91	-
H31	10 48 24.77	12 32 07.49	423	38.27	23

Table 4—Continued

Name	R.A.(2000.0)	Dec. (2000.0)	Diameter (pc)	log L (erg/sec)	HK-ID
H32	10 48 24.33	12 32 18.05	198	37.80	-
H33	10 48 24.93	12 32 01.83	704	39.01	24
H34	10 48 23.90	12 32 26.76	495	38.44	-
H35	10 48 24.83	12 31 59.72	504	38.49	-
H36	10 48 24.00	12 32 16.94	457	38.57	26
H37	10 48 24.92	12 31 52.58	239	37.82	-
H38	10 48 23.65	12 32 21.01	358	37.90	-
H39	10 48 25.33	12 31 37.57	463	38.66	27
H40	10 48 25.12	12 31 42.45	396	38.23	28
H41	10 48 24.30	12 32 01.50	880	38.91	29
H42	10 48 23.35	12 32 21.41	564	38.67	31
H43	10 48 23.82	12 32 08.01	1087	39.04	30
H44	10 48 22.92	12 32 24.08	320	38.32	33
H45	10 48 23.32	12 32 11.27	653	38.92	35
H46	10 48 24.49	12 31 40.50	285	38.05	34
H47	10 48 23.69	12 31 56.82	333	37.86	-
H48	10 48 24.32	12 31 39.84	291	38.36	38
H49	10 48 22.45	12 32 23.00	487	38.74	39
H50	10 48 22.17	12 32 19.74	442	38.09	-
H51	10 48 22.47	12 32 11.55	399	38.10	-
H52	10 48 23.03	12 31 57.23	460	38.40	41
H53	10 48 23.13	12 31 51.79	698	39.28	42
H54	10 48 22.62	12 31 58.79	270	37.70	-
H55	10 48 21.73	12 32 16.79	507	38.82	45
H56	10 48 22.63	12 31 53.63	618	38.99	46
H57	10 48 22.38	12 31 59.07	340	38.21	49
H58	10 48 21.52	12 32 19.51	308	38.08	48
H59	10 48 21.70	12 32 09.81	596	38.34	-
H60	10 48 21.52	12 32 12.48	400	38.10	50
H61	10 48 21.31	12 31 59.60	369	38.08	-